Food Chemistry 253 (2018) 71–78

Contents lists available at ScienceDirect

Food Chemistry

journal homepage: www.elsevier.com/locate/foodchem

Double emulsions as potential fat replacers with gallic acid and quercetin nanoemulsions in the aqueous phases

Wladimir Silva[a], María Fernanda Torres-Gatica[a], Felipe Oyarzun-Ampuero[b], Andrea Silva-Weiss[a], Paz Robert[b], Susana Cofrades[c], Begoña Giménez[a,*]

[a] Dpto. Ciencia y Tecnología de los Alimentos, Facultad Tecnológica, Universidad de Santiago de Chile, Santiago, Chile
[b] Dpto. Ciencia de los Alimentos y Tecnología Química, Facultad de Ciencias Químicas y Farmacéuticas, Universidad de Chile, Casilla 133, Santiago, Chile
[c] Institute of Food Science, Technology, and Nutrition (ICTAN-CSIC), Jose Antonio Novais, 10, 28040 Madrid, Spain

ARTICLE INFO

Keywords:
Oil blends
Double emulsions
Nanoemulsion
Gallic acid
Quercetin

ABSTRACT

The development of fat replacers to obtain healthier/functional foods is a constant challenge. With this aim, double emulsions (DE) with a blend of olive, linseed and fish oils as oil phase were developed. To prevent the oxidation of these oils, gallic acid and quercetin were incorporated in the internal and the external aqueous phase (W_2), respectively, according to a factorial design. Considering the low solubility of quercetin in water, it was included in O/W nanoemulsions (QN), thus being freely dispersible in W_2. The antioxidant activity in DE was attributed to QN, which significantly improved the oxidative stability of DE/QN. Furthermore, DE/QN showed good physical stability with a limited coalescence during storage at 4 °C for 28 days, significantly longer than time usually required for food ingredients. Therefore, DE/QN could be used as potential fat replacer in a variety of food formulations, providing blends of fatty acids consistent with dietary recommendations.

1. Introduction

Water-in-oil-in-water ($W_1/O/W_2$) double emulsions (DEs) are multi-compartmentalized systems where a water-in-oil (W_1/O) emulsion is dispersed as droplets within an external aqueous phase (W_2) (McClements, Decker, Park, & Weiss, 2009). Although encapsulation and controlled release of bioactive compounds is one of the main potential applications of $W_1/O/W_2$ DEs in the food industry, they may have other promising applications in foods. Thus, DEs offer the opportunity to design delivery systems for fatty acids to meet dietary recommendations for prevention of diet-related chronic diseases, namely reducing saturated fatty acids (SFA) intake and promoting the consumption of monounsaturated (MUFA) and polyunsaturated (PUFA) ω3 and ω6 fatty acids (FAO/WHO, 2010; Tressou et al., 2016). Therefore, by suitable formulation of the oil phase, DEs could be used as fat replacers in the development of healthier/functional foods with lower content of SFA and higher content of MUFA and PUFA. Several studies have been focused on the development of DEs enriched in unsaturated fatty acids to be used as functional ingredients. Vegetable oils such as olive, canola, chia, sunflower, linseed, soybean or perilla have been used as oil phase in the formulation of DEs (Jiménez-Colmenero, 2013), but blends of oils closer to health recommendations have not been yet studied.

Double emulsions designed with blends of unsaturated fatty acids may be susceptible to lipid oxidation, leading to the development of off-flavors and off-odors, together with the formation of potentially toxic compounds. Although there are many studies focused on the oxidative stability of conventional emulsions, especially oil-in-water (O/W) emulsions (Waraho, Cardenia, Decker, & McClements, 2010), research on oxidative stability of more complex emulsions such as multiple emulsions is scarce (Flaiz et al., 2016; Kiokias & Varzakas, 2017; O'Dwyer et al., 2013; O'Dwyer, O'Beirne, Ní Eidhin, & O'Kennedy, 2012; Poyato et al., 2013).

Oxidation of PUFA is a complex chemical reaction, and multiple antioxidant hurdle technologies are frequently required for their stabilization (McClements et al., 2009). Thus, the use of antioxidants is a common strategy for preventing lipid oxidation in food emulsions (Mcclements & Decker, 2000). Phenolic compounds have been widely used due to their ability to donate electrons and/or hydrogen atoms to free radicals, as well as to their capacity of chelating metal ions (Craft, Kerrihard, Amarowicz, & Pegg, 2012). The efficiency of phenolic compounds in O/W emulsions depends on several factors such as concentration, physical location, chemical structure, steric issues, nature of lipids, interactions with other components and relative polarity to the

* Corresponding author at: Facultad Tecnológica, Departamento de Ciencia de los Alimentos y Tecnología de los Alimentos, Universidad de Santiago de Chile, Avenida Libertador Bernardo O'Higgins 3363, Estación Central, Santiago, Chile.
E-mail address: bego.gimenez@usach.cl (B. Giménez).

https://doi.org/10.1016/j.foodchem.2018.01.128
Received 25 June 2017; Received in revised form 18 January 2018; Accepted 22 January 2018
Available online 03 February 2018
0308-8146/

type of lipids present in the emulsion (Espinosa, Inchingolo, Alencar, Rodriguez-Estrada, & Castro, 2015; Jayasinghe, Gotoh, & Wada, 2013; Shahidi & Zhong, 2011). The antioxidant activity of gallic acid (GA) and quercetin (Q) has not been evaluated in multiple emulsions, but they have been incorporated in O/W emulsions (Di Mattia, Sacchetti, Mastrocola, Sarker, & Pittia, 2010; Espinosa et al., 2015; Gomes, Costa, de Assis Perrechil, & da Cunha, 2016). Quercetin has structural features that impart high antioxidant activity, such as the ortho 3′,4′-dihydroxy moiety in the B-ring, and the 2,3-double bond in combination with both a 4-keto group and a 3-hydroxyl group in the C ring (Heim, Tagliaferro, & Bobilya, 2002). However, one of the main disadvantages of using Q in functional foods is its low solubility in aqueous and oil media. Regarding this, several strategies have been used to increase the solubility/dispersability and bioavailability of Q, such as nanoemulsification, complexation with cyclodextrins or liposome encapsulation (Karadag, Yang, Ozcelik, & Huang, 2013).

The multi-compartmentalized structure of DEs offers the opportunity to incorporate antioxidants in different locations, thus potentially obtaining synergic effect due to the presence of antioxidants with different solubility and antioxidant mechanism. The aim of this study was to design DEs as delivery systems for blends of healthy fatty acids, with Q incorporated in the W_2 and GA in the internal aqueous phase (W_1). To overcome the disadvantage of the low solubility of quercetin in water, quercetin O/W nanoemulsions (QN) were developed as nanocarriers for Q in DE and they were dispersed in W_2. In contrast with most of the works addressing oxidative stability in emulsions, where effective antioxidant concentrations are determined through assay and error studies, we propose a factorial design to optimize the concentrations of GA and Q in DE. DEs obtained under optimal conditions were evaluated for droplet size, morphology and stability. Furthermore, their oxidative stability was evaluated under accelerated conditions.

2. Materials and methods

2.1. Materials

Double emulsions: Olive oil (Team Foods S.A., Chile), linseed oil (Nutra Andes Ltda., Chile) and fish oil (SPESS S.A., Chile). Polyglycerol ester of polyricinoleic acid (PGPR; Dimerco S.A., Chile), sodium caseinate (Prinal S.A., Chile), gallic acid (Sigma-Aldrich, Chile). Nanoemulsions: Miglyol 812 (neutral oil formed by esters of caprylic and capric fatty acids and glycerol, Sasol GmbH, Germany), Epikuron 145 V (phosphatidylcholine-enriched fraction of soybean lecithin, Cargill, Spain), ethanol (Merck, Chile). Quercetin was acquired from Sigma-Aldrich (Chile).

2.2. Fatty acid profile of the oil blend

A blend of olive, linseed and fish oils (70:20:10) was designed in previous studies (data not shown) and used as lipid phase in the formulation of DE. Fatty acid methyl esters (FAMEs) were prepared according to UNE-EN ISO 5509:2001. FAMEs were analyzed using a gas chromatograph (7890B, Agilent, Chile) fitted with a fused-silica capillary column (HP-88, 100 m × 0.25 mm i.d. × 0.20 μm film thickness) and a flame ionization detector. The injector and detector temperatures were set at 250 °C, and the hydrogen flow at 1 mL/min. The initial oven temperature was 180 °C, held from 20 min, and increased to 215 °C at a rate of 2 °C/min, held for 15 min. The injection volume was 0.5 μL. FAME standards (GLC 569, Nu-Chek Prep. Inc., USA) were used to identify the fatty acids, and tricosanoic acid was used as internal standard. The results were expressed as percentage of methyl esters. The determination was performed in triplicate.

2.3. Preparation of quercetin nanoemulsions

A quercetin O/W nanoemulsion (QN) was prepared by the solvent evaporation method according to Lozano et al. (2008), with some modifications. Briefly, Epikuron 145 V (600 mg) and quercetin (281 mg) were dissolved in ethanol (10 mL). Then, Miglyol 812 (2.5 mL) was added to the above solution, which was then verted into 190 mL of ethanol. Finally, this ethanolic phase was added to an aqueous phase (400 mL) and the final mixture was rotaevaporated to a final volume of 50 mL.

2.3.1. Characterization of quercetin nanoemulsions

The size and zeta potential of the QN was determined by photon correlation spectroscopy and laser Doppler anemometry, with a Zetasizer Nano-ZS (Malvern Instruments, UK). The concentration of Q in the O/W nanoemulsion was quantified by dissolving an aliquot of the nanosuspension in acetone (1:500) and the absorbance was measured in a UV–Vis spectrophotometer (Aquamate 8000, Orion, USA) at 370 nm. The standard calibration curve of quercetin was linear (0–10 μg/mL; $R^2 = 0.99$) in the range of tested concentrations (molar extinction coefficient 0.102 M^{-1} cm^{-1}). Scanning transmission electron microscopy (STEM) images were obtained to analyze the morphology of the carriers. The samples for STEM were prepared by depositing one droplet (10 μL) of the nanoemulsion, one droplet of MilliQ-water and one droplet of phosphotungstic acid (1%) on a Parafilm™ surface. Then, a copper grid (200 mesh, covered with Formvar) was incubated with each droplet for 2 min, and allowed to dry for 4 h. The association efficiency of Q in the nanocarriers was determined by calculating the difference between the total content of Q in the O/W nanoemulsion (obtained after the rotaevaporation) and that obtained in the continuous aqueous phase of the O/W nanoemulsion. Thus, the nanoemulsion was centrifuged (6000*g*, 10 min) to separate the continuous aqueous phase using VIVASPIN® tubes (100 kDa MWCO). The concentration of Q in the continuous phase was measured spectrophotometrically as described above. All the determinations were performed on three different nanoformulations.

2.4. Preparation of double emulsions

Double emulsions were formulated following a two-step emulsification process (Cofrades, Antoniou, Solas, Herrero, & Jiménez-Colmenero, 2013). GA was dissolved in W_1 (2–225 mg GA/kg DE) and QN was dispersed in W_2 (2–225 mg Q/kg DE). Furthermore, a control DE without GA and QN was prepared for comparative purposes (DE/C). In all the emulsions, the osmolarity of W_1 and W_2 was determined using an osmometer (3320, Advanced Instruments, USA) and equilibrated using NaCl to prevent diffusion phenomena. PRPG (lipophilic emulsifier) was added to the oil blend used as lipid phase (6% w/w). A W_1/O coarse emulsion was prepared by drop-wise addition of W_1 (20%) to the oil phase (80%) using a blender (Thermomix, Vorwek, Germany; 3250 rpm, 5 min, 50 °C). The coarse emulsion was homogenized twice with a two-stage high pressure homogenizer (Panda Plus 2000, GEA Niro Soavi, Italy) at 7977 psi (first stage) and 1015 psi (second stage). The W_1/O/W_2 coarse emulsion was prepared by gradually addition of the primary W_1/O emulsion (40%) to W_2 (60%) with sodium caseinate as hydrophilic emulsifier (0.5% w/w), followed by mixing (700 rpm, 5 min, room temperature). This coarse emulsion was homogenized twice at 2175 psi (first stage) and 435 psi (second stage). The main steps of the preparation of DE with GA and QN are shown as Supplementary material.

A three-level factorial design with 11 runs and two blocks was performed to optimize the GA content in the internal aqueous phase (W_1) and QN content in the external one (W_2). The concentrations of GA (2–225 mg GA/kg DE) and Q (2–225 mg Q/kg DE) were evaluated as independent variables. The dependent variable was lipid oxidation, evaluated as thiobarbituric acid reactive substances (TBARS) and expressed as induction time (IT_{TBARS}, time elapsed until TBARS curves showed an inflection point). Data were fitted to a polynomial function (time/MDA ratio vs. time) and the maximum point of polynomial

function was obtained applying first derivative. All the experiments were performed randomly to avoid systematic bials. The data were fitted to a second-order regression model, according to Eq. (1).

$$Y = b_0 + \sum_{i=1}^{2} b_i X_i + \sum_{i=1}^{2} b_{ii} X_i^2 + \sum_{i=1}^{1} \sum_{j=i+1}^{2} b_{ij} X_i X_j \quad (1)$$

where Y was the estimated response, subscript i and j ranged from 1 to the number of variables (n = 2), b_0 was the intercept term, b_i values were the linear coefficients, b_{ii} values were the quadratic coefficients, b_{ij} values were the interaction coefficients, and X_i and X_j were the levels of independent variables.

The analysis of variance (ANOVA), test of lack of fit, and determination of regression coefficients were performed with the software Statgraphics (5.0 program, Manugistics Inc., Rockville, MA). RSM was applied to maximize the response variable. Non-significant terms ($p < .05$) were removed from the equation, but when the quadratic and/or cross-product forms were significant, the linear form was considered in the model, although the linear form was not significant because they are fundamental elements of the mathematical model (Romero & Zuñica, 2005).

2.5. Measurement of interfacial tension

The interfacial tension at the inner (W_1-O) and outer (O-W_2) interfaces of DEs was determined by the pendant drop method (Skurtys & Aguilera, 2009). Briefly, small drops (10–30 μL) of the W_1 and W_2 were attached to the tip of a stainless-steel needle (outer diameter 1.25 ± 0.005 mm) (Sigma-Aldrich, St. Louis, USA) and hanged into the oil phase under constant temperature (20 ± 1 °C). The drop was formed by a controlled syringe pump (NE-1000, New Era Pump System Inc., NY, USA). Images of the drop (100 images) were taken at equilibrium state with a high-speed charge-coupled device (CCD) camera (Pulnix Model TM-6740GE, Pulnix Inc., CA, USA), equipped with a zoom objective and operated via software. The shape of the drop at equilibrium results from the balance of gravity and interfacial tension, being possible to use the fundamental Laplace equation, as reported by Skurtys and Aguilera (2009), to determine the interfacial tension. To validate the results, it was corroborated experimentally that interfacial tension of pure water/air system was 72.3 mN m^{-1}.

2.6. Encapsulation efficiency

The encapsulation efficiency (EE) of GA in DEs was determined immediately after preparation by measuring the GA concentration in W_2 by HPLC according to Robert, García, Reyes, Chávez, and Santos (2012), using a Merck Hitachi L-6200 pump, a Waters 996 photodiode-array detector and a C18 column (3 μm, 4.6 i.d. × 150 mm, Waters, Ireland). A 4-fold dilution of DEs in water with the adjusted osmolarity was centrifuged (2500*g*, 30 min) to separate oil globules from the W_2, filtered (0.22 μm, Millipore filter), and injected into the HPLC. The EE was defined as the percentage of GA in W_1 that remained in the primary emulsion W_1/O after the second emulsification process and calculated following the equation (2):

$$EE = 100 - \frac{GA_{W2}x100}{GA_t} \quad (2)$$

where GAW_2 is GA concentration recovered in W_2, GAt is the total concentration added to W_1.

2.7. Characterization and stability of DEs obtained under optimal conditions

2.7.1. Measurement of droplet size and size distribution

The particle size and distribution of oil droplets in DEs were determined using a Malvern Mastersizer 3000 particle size analyzer (Malvern Instrument Ltd., Worcestershire, UK), equipped with a He-Ne laser (λ = 633 nm) and a measurement range 0.02–2000 μm. Particle size calculations were based on the Mie Scattering theory. Ten measurements were performed on each emulsion. The results were expressed as the average of the volume-weighted mean globule size ($D_{[4,3]}$).

2.7.2. Confocal laser scanning microscopy

Morphology of DEs was evaluated by confocal laser scanning microscopy (CLSM, LSM 700, Carl Zeiss, Germany) at 40x and 100x magnifications. The oil phase of DEs was fluorescently labelled with Nile red (0.02% w/w). Samples were placed onto microscope slides, covered with a cover glass and subjected to 488 nm excitation wavelength, while fluorescent signal was collected at 580 nm. The software used for the CLSM imaging was ZEN 2012 (Blue Edition, Carl Zeiss, Germany).

2.7.3. Emulsion stability

Emulsion stability of DEs was evaluated using a vertical scan analyzer (Turbiscan MA2000, Formulation, France), consisted on a pulsed near-IR light source (λ = 850 nm) and two synchronous detectors (transmission and backscattering). Emulsions were poured into the test cells (total height 60 mm) and the physical phenomena of destabilization were evaluated through the backscattering (BS) profiles as a function of the sample height in the test cells for 28 days at 4 °C. Creaming index (CI) was calculated from the BS profiles according to the following equation (Eq. (3)):

$$Creaming\ Index = \frac{HS}{HE} \times 100 \quad (3)$$

where HS is the height of the serum layer and HE is the total height of the emulsion.

2.7.4. Lipid oxidation under accelerated conditions

Double emulsions were subjected to an accelerated oxidation study at 60 ± 1 °C, under standardized conditions as described by Poyato et al. (2013). Samples (in triplicate) were periodically removed to determine hydroperoxides and TBARS.

2.7.4.1. Hydroperoxides. The content of hydroperoxides was measured according to (Matalanis, Decker, & McClements, 2012). Briefly, 1 mL of DE was vortexed three times for 30 s with 7.5 mL of chloroform:methanol (2:1 v/v), followed by centrifugation (1300*g*, 5 min). Afterwards, 200 μL of the chloroform/methanol layer was mixed with 2.8 mL of methanol/1-butanol (2:1 v/v). Then, 15 μL of ferrous iron solution (prepared by mixing 132 mM barium chloride and 144 mM ferrous sulphate) and 15 μL of 3.94 M ammonium thiocyanate were added to the mixture and allowed to react in the dark for 20 min at room temperature. The absorbance of the samples was measured at 510 nm using a spectrophotometer (Aquamate UV–Vis, Thermo Fisher Scientific, USA). The results were expressed as mmol cumene hydroperoxide/kg oil, according to a standard curve of cumene hydroperoxide (0–20 μM; $R^2 = 0.99$).

2.7.4.2. TBARS. TBARS were determined as described by Poyato et al. (2013) with slight modifications. Briefly, an aliquot of DE (0.5 g) was mixed with 0.5 mL of distilled water, 20 μL of BHT (1% w/v) and 2 mL of the TBARS reagent (15% w/v trichloroacetic acid and 0.0375% w/v 2-thiobarbituric acid in 0.25 N HCl). The mixture was vortexed, placed in boiling water (15 min) and cooled down to room temperature in an ice bath. Hexane (1 mL) and ammonium sulphate (1 mL, 4 M) were added to the mixture, vortexed and centrifuged (1700*g*, 10 min, 20 °C). The absorbance of the supernatant was measured at 532 nm and the results were expressed as mg of malondialdehyde (MDA)/kg DE, according to a calibration curve obtained using 1,1,3,3-tetraethoxypropane (0–25 μM; $R^2 = 0.99$).

Table 1
Fatty acid composition of the oil blend.

Fatty acid	Oil blend[†] (%)[*]
C14:0	0.69 ± 0.01
C16:0	11.14 ± 0.10
C18:0	2.43 ± 0.04
C21:0	0.28 ± 0.01
Other SFA	0.29 ± 0.01
C16:1	1.41 ± 0.01
C18:1n-9	55.14 ± 0.34
C18:1n-7	2.14 ± 0.02
Other MUFA	0.10 ± 0.14
C18:2n-6	9.69 ± 0.06
C18:3n-6	0.34 ± 0.01
C18:3n-3	12.21 ± 0.09
C20:5n-3	1.60 ± 0.01
C22:5n-3	0.23 ± 0.01
C22:6n-3	1.06 ± 0.03
Other PUFA	0.60 ± 0.01
ΣSFA	**14.83 ± 0.15**
ΣMUFA	**58.79 ± 0.31**
ΣPUFA	**25.73 ± 0.10**
Σn-3	15.10 ± 0.03
Σn-6	10.03 ± 0.06
PUFA/SFA	1.73

[*] Expressed as percentage of methyl ester.
[†] Olive:linseed:fish oil (70:20:10).

2.7.5. Statistical analysis

The reported results correspond to the arithmetic mean of three batches ± standard deviation. One-way variance analyses were carried out to establish significant differences between values obtained for the same sample. The differences of means between samples were resolved by confidence intervals using Fisher Least Significant Difference (LSD) test (Statgraphics 5.0 program, Manugistics Inc., Rockville, MA). The level of significance was set for $p \leq .05$.

3. Results and discussion

3.1. Fatty acid profile of the oil blend

Table 1 shows the fatty acid composition of the oil blend (olive:-linseed:fish oil 70:20:10) used as oil phase in DEs. Five fatty acids comprised about 90% of the total fatty acids analyzed in the oil blend: palmitic, stearic, oleic, linoleic and linolenic acids. The major fatty acid was oleic acid (55%), whereas the total MUFA content was 59%. This oil blend was low in SFA (15%) and rich in PUFA (26%), with 15% ω3 (2.66% EPA + DHA) and 10% ω6, in line with dietary recommendations. Given that the fat content in the double emulsion was 30.8%, the PUFA content was approximately 7.92%, containing 3.76% of linolenic acid and 0.82% of EPA + DHA. The use of DEs designed with this oil blend as animal fat replacer in the formulation of healthier or functional foods such as meat-based foods, would allow noticeable reductions in the SFA content together with higher proportions of PUFA, in line with dietary recommendations (FAO/WHO, 2010; Tressou et al., 2016). SFA and PUFA levels reported for pork back-fat, usually used in the formulation of meat-based products, are around 36% and 14%, respectively (Rodríguez-Carpena, Morcuende, & Estévez, 2012). According to several studies focused on the intake of fatty acids in general populations worldwide, higher SFA and lower PUFA intakes (especially long chain ω3 PUFA) than those recommended are reported in many countries (Harika, Eilander, Alssema, Osendarp, & Zock, 2013; Tressou et al., 2016). Furthermore, lower intakes of SFA are not usually accompanied by higher intakes of PUFA (Harika et al., 2013), as recommended to reduce many risk factors involved in the development of cardiovascular diseases.

Delgado-Pando, Cofrades, Ruiz-Capillas, Solas, and Jiménez-Colmenero (2010) designed an oil blend to be used as oil phase in O/W emulsions that were incorporated in the formulation of meat based products as pork back-fat replacers. This oil blend was composed of olive (44.39%), linseed (37.87%) and fish (17.74%) oils, and showed contents of SFA, MUFA and PUFA around 16%, 47% and 36%, respectively. The main advantage of using DEs over conventional O/W emulsions as fat replacers is that part of the lipid material is replaced by water in DE, allowing a significant reduction in the fat content besides the improvement of the lipid profile, but maintaining the physicochemical and sensory properties (McClements et al., 2009).

3.2. Quercetin nanoemulsions

Considering the low solubility of Q in water (0.17–7.7 μg/mL; Karadag et al., 2013), its direct addition into the external aqueous phase of the multiple emulsion was not possible due to formation of precipitates. Thus, Q was included into the oil phase of an O/W nanoemulsion prepared by the solvent evaporation method. The nanoemulsification process is spontaneously induced using this strategy, avoiding high energy steps that is an advantage compared with other nanoformulations containing Q (Ebrahimi & Salmanpour, 2014; Gonçalves et al., 2015; Karadag et al., 2013). The QN was in a nanometric range of 189 ± 12 nm and showed low polydispersity (between 0.1 and 0.2). The above results could be contrasted with the STEM images (Supplementary material), which also evidenced spherical nanoemulsions. The nanoformulations showed negative zeta potential (−46 ± 5 mV), attributed to the presence of Epikuron 145 V (mixture of surfactants that include zwitterionic phospholipids, anionic fatty acids, and phosphatidic acid, among others), and whose magnitude refers to stable systems (Orellana, Torres-Gallegos, Araya-Hermosilla, Oyarzun-Ampuero, & Moreno-Villoslada, 2015). The oil nucleus in the O/W nanoemulsion entrapped 96.5 ± 0.5% of Q.

3.3. Incorporation of GA and QN in DE

A three-level factorial design was performed to optimize the concentrations of GA and QN, incorporated in W_1 and W_2, respectively. The experimental design for the incorporation of GA and QN is shown as Supplementary material. RSM was applied to optimize the response variable (IT_{TBARS}), considering linear, quadratic and cross-product forms of the independent variables at 95% confidence level. The analysis of variance (ANOVA) is shown as Supplementary material.

The IT_{TBARS} values ranged from 1 to 21 days. The linear and quadratic forms of the concentration of Q, and the interaction between concentration of Q and GA were significant for IT_{TBARS}, whereas the linear and quadratic concentration of GA were not significant. The model explained the 92.0% of the variability (R-squared adj. for d.f.) in IT_{TBARS}, and the residual values were below 6.0. The quadratic regression equation describing the effect of the independent variables on IT_{TBARS}, after removing the non-significant terms, is the following:

$$IT_{TBARS} = 1.83718 + 0.13576^{*}[Q] + 0.03403^{*}[GA] - 0.000204^{*}[Q]^2 - 0.00024^{*}[Q]^{*}[GA]$$

Although lack of fit may occur when quadratic or cross-product terms are not included in the model (Meddour, Yallese, & Aouici, 2015), the lack of fit remained not significant ($p > .05$) in this study after the quadratic form of concentration of GA was removed from the model (ANOVA is shown as Supplementary material).

The optimization of the concentrations of GA and QN in DE had the objective of maximizing the response variable (IT_{TBARS}). The optimum value for IT_{TBARS} was 22 days, obtained with 2 mg GA and 225 mg Q/kg DE. Fig. 1 shows the response surfaces obtained for IT_{TBARS}. According to this figure, in the range of concentrations studied, high concentrations of Q and low concentrations of GA extended IT_{TBARS}. Thus, with the minimum concentration of GA, the increase in Q concentration led to an increase of 20 days in IT_{TBARS}. It is known the high antioxidant

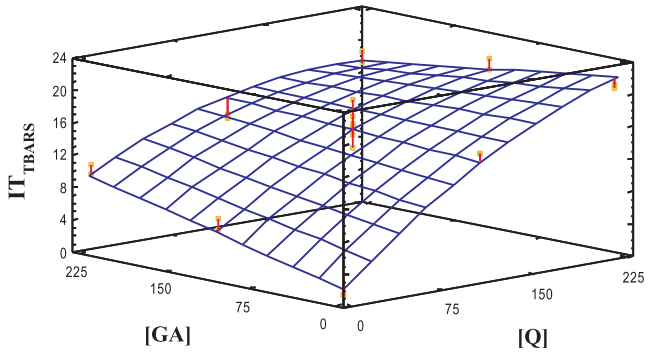

Fig. 1. Response surface graphs for IT_{TBARS} in DEs with gallic acid and quercetin nanoemulsions.

activity of quercetin. However, Q has limited solubility in water and therefore it was included nanoencapsulated in W_2. Using this strategy, concentrations of quercetin as high as 375 μg Q/mL of W_2 could be achieved in those experimental runs with the highest level of Q. Free radicals are generated during lipid oxidation of oils, and in the case of emulsion systems, these radicals are able to locate at the oil-water interface, where Q acts as antioxidant by donating a hydrogen and/or an electron to the peroxyl radicals and/or other free radicals, whereas the flavonoid radicals formed are stabilized by resonance (Heim et al., 2002). This mechanism would involve that QN was able to locate also at the oil-water interface to exert its antioxidant effect, as will be discussed below. To the best of our knowledge, this is the first study where an antioxidant is included in an O/W nanoemulsion and dispersed in the aqueous phase of a DE, highlighting the high oxidative stability that this strategy provides to DE.

Only a slight increase in IT_{TBARS} value was obtained with increasing GA concentrations in the range studied (Fig. 1), showing a low antioxidant effect. The W_1 of DEs showed pH values below 4.0 in the range of GA concentrations used in this study. At this pH value, the encapsulated GA (EE over 80% in all the experimental runs, data non-shown) would be present in both its neutral and monoanionic form (pK_a of the carboxylic acid group = 4.3), with a predominance of the neutral form that can be distributed between the internal aqueous phase and the W_1-O interface (Losada-Barreiro, Bravo-Díaz, & Romsted, 2015), but unable to migrate towards the O-W_2 interface, where lipid oxidation mainly takes place in emulsion systems (Mcclements & Decker, 2000), due to GA is essentially insoluble in oil (Losada-Barreiro, Sánchez-Paz, Bravo-Díaz, Paiva-Martins, & Romsted, 2012). Poyato et al. (2013) reported that the antioxidant effect of a hydrophilic antioxidant (aqueous *Melissa* extract) encapsulated in W_1 of linseed oil DEs was lower than that of butylated hydroxyanisole (BHA), possibly because BHA was slowly released to the oil phase due to its lipophilic nature, whereas the aqueous *Melissa* extract mainly remained in W_1. Regarding unencapsulated GA, this will be fully deprotonated since the pH value of W_2 was in the range 7.0–7.3, and therefore mostly located in the W_2, explaining its limited antioxidant effect.

Acidity (pH of the aqueous phase of the emulsion), among other factors such as emulsifier concentration and temperature, has been reported to control the distribution of GA in an O/W emulsion, and therefore its antioxidant efficiency. Food emulsion pH may change the partitioning of GA between interfacial and aqueous region, since this antioxidant will be partially ionized depending on pH value (Losada-Barreiro et al., 2015, 2012).

Given that the response variable (IT_{TBARS} value) was maximized with the minimum concentration of GA in W_1 and the maximum concentration of QN in W_2, DEs without GA in W_1 and the optimal concentration of QN in W_2 (DE/QN) were prepared and the IT_{TBARS} was determined to elucidate the contribution of GA to the antioxidant efficiency observed. As expected, there were not significant differences ($p > .05$) in IT_{TBARS} value between DE/GA-QN and DE/QN (data non-shown). Therefore, DE/QN was chosen for further studies. DE/C and DE/QN were stored at 4 °C for 30 days, and the droplet size and size distribution, morphology and stability were periodically evaluated. Furthermore, their oxidative stability was evaluated under accelerated conditions.

3.4. Measurement of interfacial tension

The interfacial tension at the inner (W_1-O) and outer (O-W_2) interfaces of DEs was determined by the pendant drop method. The equilibrium interfacial tension of the oil blend-water system was 16.12 ± 0.91 mN m^{-1}. In the W_1-O interface, the addition of GA to the W_1 led to a small but significant decrease ($p \leq .05$) of the interfacial tension (14.27 ± 0.25 mN m^{-1}), indicating that GA is able to locate at the interface as suggested above. Di Mattia, Sacchetti, Mastrocola, and Pittia (2009) also reported that GA was able to decrease interfacial tension of an olive oil-water interface. In contrast, Gomes et al. (2016) reported that the addition of GA to water (0.5% w/w) did not have any effect on the interfacial tension of a soybean oil-water system. As expected, the interfacial tension of the oil blend-GA system significantly decreased ($p \leq .05$) after the addition of PGPR to the oil (6% w/w), reaching values of 5.57 ± 0.12 mN m^{-1}. Higher reduction of the interfacial tension has been reported when PGPR is used as emulsifier in W/O or DE emulsions (Gomes et al., 2016; Weiss & Muschiolik, 2007). The efficiency of PGPR as lipophilic emulsifier may be affected by the oil type and/or other minor compounds in oil (Weiss & Muschiolik, 2007). Regarding the O-W_2 interface, the incorporation of the QN into the W_2 led to a significant reduction in the values of interfacial tension (10.60 ± 0.30 mN m^{-1}; $p \leq .05$), when compared with those of the oil blend-water system (16.12 ± 0.91 mN m^{-1}), suggesting that QN is able to locate at the oil-water interface, allowing Q to exert its antioxidant activity. The incorporation of the hydrophilic emulsifier (sodium caseinate, 0.5% w/w) to the Q-nanoemulsion dispersed in water to provide the W_2, significantly decreased ($p \leq .05$) the interfacial tension to values of 4.80 ± 0.28 mN m^{-1}.

3.5. Characterization and stability of DEs with optimal concentration of QN (DE/QN)

3.5.1. Measurement of droplet size and size distribution

Fig. 2 shows the droplet size distribution of DE/C and DE/QN during 28 days of storage at 4 °C. Initially, DE/C showed a monomodal size distribution with sizes between 0.2 and 16 μm, whereas DE/QN showed a dominant distribution ranging from 0.2 to 10 μm and a small distribution between 10 and 100 μm. Consequently, DE/C showed lower $D_{[4,3]}$ values than DE/QN ($p \leq .05$; Table 2). Monomodal and bimodal size distributions have been reported for similar DEs where PGPR and sodium caseinate were used as emulsifiers (Bou, Cofrades, & Jiménez-Colmenero, 2014; Cofrades et al., 2014; Flaiz et al., 2016). Droplet size and size distribution in DEs may be influenced by several factors such as processing conditions, type and concentration of emulsifiers, composition of the oil phase and viscosity of the phases (Lamba, Sathish, & Sabikhi, 2015; McClements, 2016), making difficult to compare results among studies. In DEs using PGPR and sodium caseinate as emulsifiers but different oil phase, and prepared under similar conditions, initial $D_{[4,3]}$ values were in the range of 2.22–3.77 μm (Bou et al., 2014; Cofrades et al., 2013, 2014; Flaiz et al., 2016).

Storage of DEs at 4 °C produced some changes in the oil globule size distribution of both DEs, namely an increase in oil globule population with sizes over 10 μm and 100 μm for DE/C and DE/QN, respectively, possibly due to coalescence of the oil globules (Fig. 2). Although DE/C showed significantly lower $D_{[4,3]}$ values than DE/QN during the storage, denoting a higher stability, > 92% of the globule population had sizes below 10 μm in both DEs at the end of the storage time (day 28). The minor increase in size throughout the storage led to an increase of $D_{[4,3]}$ values in both DEs ($p \leq .05$), especially in the case of DE/QN

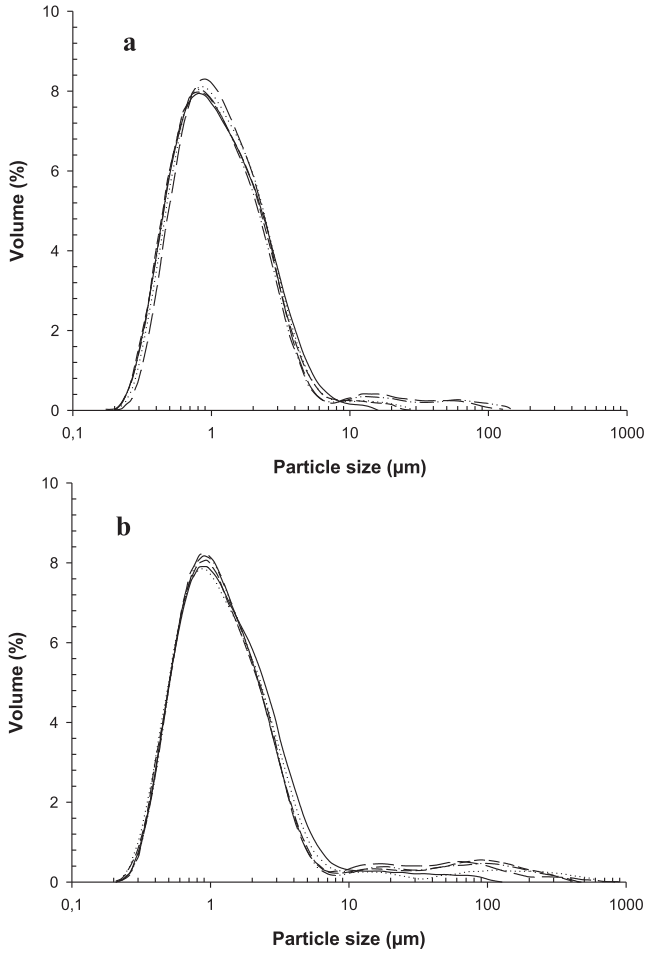

Fig. 2. Size distribution for DE/C (2a) and DE/QN (2b) during storage at 4 °C for 28 days. Day 0 (—), day 7 (·····), day 14 (- - -), day 21 (–···), day 28 (––).

Table 2
$D_{[4,3]}$ values and Creaming Index (CI) for DE/QN and DE/C during storage at 4 °C.

Time (days)	$D_{[4,3]}$ (μm)		Creaming index (%)	
	DE/QN	DE/C	DE/QN	DE/C
0	2.47 ± 0.08^{ax}	1.49 ± 0.00^{ay}	3.55 ± 0.28^{ax}	3.86 ± 0.22^{ax}
7	6.36 ± 1.24^{bx}	1.58 ± 0.01^{by}	7.16 ± 0.49^{bx}	6.51 ± 0.01^{bx}
14	8.65 ± 0.83^{cx}	1.53 ± 0.03^{aby}	11.15 ± 0.84^{cx}	9.43 ± 0.33^{cy}
21	7.64 ± 0.54^{dx}	2.83 ± 0.07^{dy}	16.15 ± 0.62^{dx}	12.36 ± 0.66^{dy}
28	7.41 ± 0.99^{dx}	2.61 ± 0.17^{cy}	17.14 ± 0.19^{dx}	14.96 ± 0.35^{ey}

Different letters (a-e) in each column mean significant differences among sampling days ($p \leq .05$).
Different letters (x-y) in each row mean significant differences between emulsions for the same sampling day ($p \leq .05$) in $D_{[4,3]}$ and creaming index, respectively.

(Table 2) since $D_{[4,3]}$ is sensitive to the presence of large particles within a polydisperse system (McClements, 2016).

3.5.2. Confocal laser scanning microscopy

Fig. 3 shows the microscopic structure of DE/C and DE/QN at day 0 and day 28 of storage at 4 °C. Both emulsions showed the typical compartmentalized structure of double emulsions, with small water droplets inside the oil globules. Moreover, some larger oil droplets can be observed in both DE/C and DE/QN at day 28 of storage, due to the coalescence of the oil globules, which correlates with the evolution observed in droplet size throughout storage. Furthermore, larger inner water droplets can be observed both in DE/C and DE/QN at the end of the storage time, suggesting that coalescence of the inner water droplets also occurred.

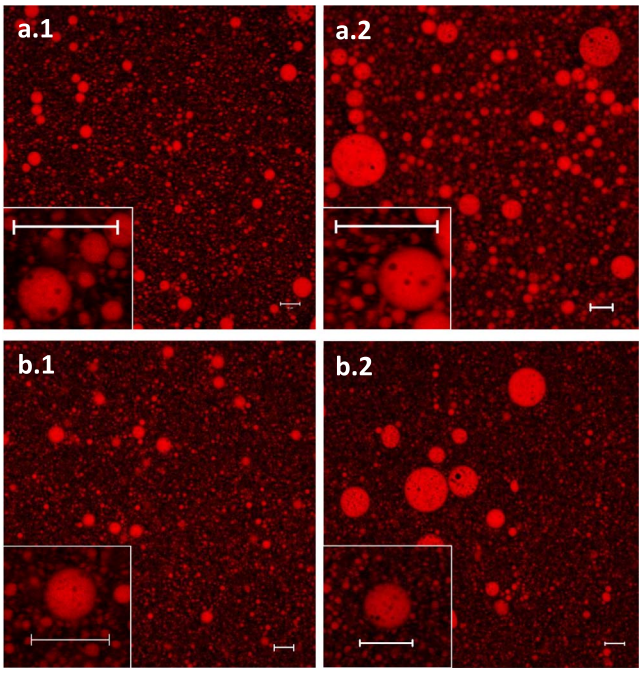

Fig. 3. CLSM images for DE/C and DE/QN. a.1: DE/C day 0; b.1: DE/C day 28; a.2: DE/C day 28; b.2: DE/QN day 28. Scale bar represent 10 μm at 40x and 100x magnifications.

3.5.3. Emulsion stability

Table 2 shows the creaming index (CI) for both DE/C and DE/QN during the storage at 4 °C. Initially, both DEs showed similar values of CI ($p > .05$), in the range 3.55–3.86%. In general, there were small changes in BS profiles of both DEs with storage time (Supplementary material), indicating its high stability. A clarification process was observed at the bottom of the cells in both DEs with storage time, due to the lower density of oil droplets that rise towards the top of the cell (Matos, Gutiérrez, Iglesias, Coca, & Pazos, 2015), leading to the increase of CI values. DE/QN showed the highest increase in CI values, and significant differences were found between both DEs from day 7 of storage ($p \leq .05$). Furthermore, in the case of DE/QN, the levels of BS in the middle of the sample decreased by about 7% from day 14 of storage, suggesting limited coalescence of the oil droplets, in accordance with the previous results of droplet size and CLSM images. In contrast, DE/C showed more stable BS profiles, and the level of BS was over 95% throughout the storage.

The instability of DEs due to creaming has been determined visually by measuring the serum layer separation in most of the studies (Bou et al., 2014; Cofrades et al., 2013, 2014). However, the visual assessment is not as accurate as using a vertical scan analyzer since the turbidity of the serum layer can make it difficult to determine its height, and the CI values may be underestimated.

3.5.4. Lipid oxidation under accelerated conditions

Fig. 4 shows the content of hydroperoxides (Fig. 4a) and TBARS values (Fig. 4b) in DE/C and DE/QN under accelerated conditions. As expected, DE/C showed higher hydroperoxide levels than DE/QN. The protective effect of QN was noticeable during storage, since significant differences were found between both DEs ($p \leq .05$) from day 12 of storage.

The preparation of the DEs involves mechanical stress and heating (50 °C), leading to the formation of secondary oxidation products (measured by TBARS) from the decomposition of existing hydroperoxides in the oil blend during the initial two days of storage, as can be seen in Fig. 4b. Other studies (Cofrades et al., 2014; Poyato et al., 2013)

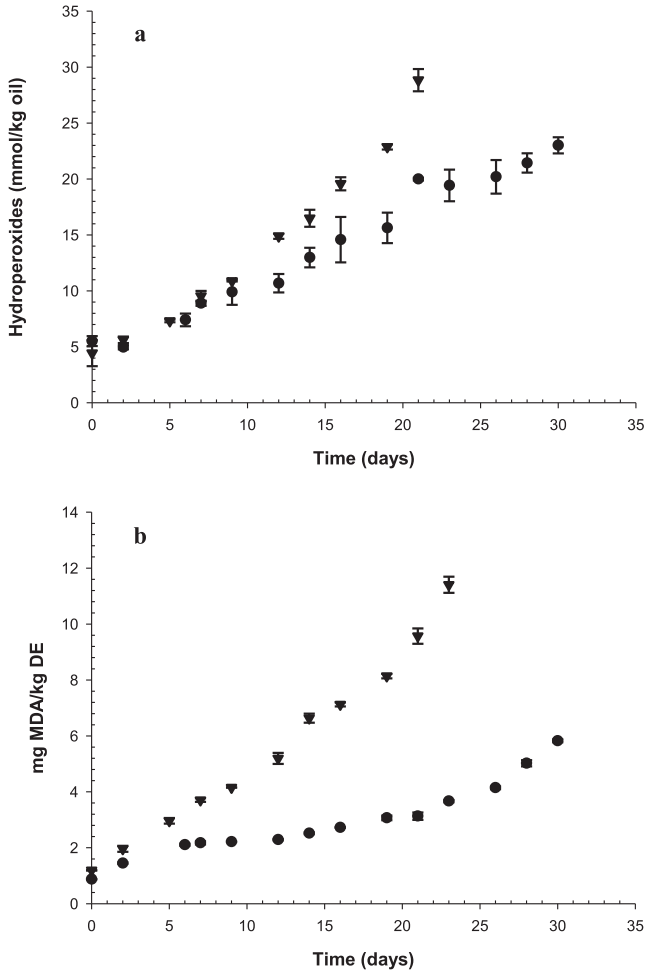

Fig. 4. Hydroperoxide formation (4a) and TBARS values (4b) for DE/C (▼) and DE/QN (●) during storage at 60 °C for 30 days.

also reported that preparation of DEs slightly increased the TBARS values, highlighting the importance of protecting the oil phase of DEs with antioxidants, especially when this consists of a blend enriched in polyunsaturated fatty acids. In the case of DE/C, a linear increase of TBARS values was observed from the beginning of the storage. However, two zones can be distinguished in the evolution of TBARS values for DE/QN (Fig. 4b). In the first zone, the TBARS values increased slightly until reaching an inflection point, from which the formation of secondary oxidation products increased, corresponding to the second zone. The IT_{TBARS} value (inflection point) for DE/QN was 21.3 days, close to values predicted by the model. To the best of our knowledge, the antioxidant activity of Q has not been previously evaluated in multiple emulsions, but this flavonoid has proven to be an effective antioxidant in O/W emulsion systems. Thus, a significant reduction in lipid oxidation has been reported when quercetin was incorporated in 20% olive oil and 10% cottonseed oil O/W emulsions emulsified by Tween (Di Mattia et al., 2010; Kiokias & Varzakas, 2014). In other study, quercetin reduced lipid oxidation evaluated by both hydroperoxides and TBARS in highly polyunsaturated O/W emulsions based on *Echium* oil and plant sterols (Espinosa et al., 2015). These authors suggested that quercetin was able to transfer hydrogen atoms or electrons to free radicals together with chelate metal ions in the aqueous phase or oil-water interface.

4. Conclusions

The development of a potential fat replacer, rich in polyunsaturated acids, has being addressed for the improvement of nutritional quality of foods. Quercetin was included in O/W nanoemulsions to allow its aqueous dispersibility in W_2, achieving concentrations of Q that significantly increased the oxidative stability of double emulsions. Furthermore, DE/QN showed a good physical stability evaluated with a variety of methods (particle size, CLSM images and backscattering profiles), with a limited coalescence during storage at 4 °C during 28 days, longer than time required for this type of food ingredients. These formulations are promising to be used as potential fat replacers in variety of products while providing fatty acid profiles consistent with dietary recommendations.

Conflict of interest

This article represents the authors own work and we are not aware of any conflict of interest.

Acknowledgements

The authors would like to thank FONDECYT 1150835 (Conicyt – Chile) and DICYT-USACH. F. O-A acknowledges to FONDECYT 1161450 and FONDAP 15130011.

Appendix A. Supplementary data

Supplementary data associated with this article can be found, in the online version, at http://dx.doi.org/10.1016/j.foodchem.2018.01.128.

References

Bou, R., Cofrades, S., & Jiménez-Colmenero, F. (2014). Physicochemical properties and riboflavin encapsulation in double emulsions with different lipid sources. *LWT – Food Science and Technology, 59*(2, Part 1), 621–628.

Cofrades, S., Antoniou, I., Solas, M. T., Herrero, A. M., & Jiménez-Colmenero, F. (2013). Preparation and impact of multiple (water-in-oil-in-water) emulsions in meat systems. *Food Chemistry, 141*(1), 338–346.

Cofrades, S., Santos-López, J. A., Freire, M., Benedí, J., Sánchez-Muniz, F. J., & Jiménez-Colmenero, F. (2014). Oxidative stability of meat systems made with W1/O/W2 emulsions prepared with hydroxytyrosol and chia oil as lipid phase. *LWT – Food Science and Technology, 59*(2), 941–947.

Craft, B. D., Kerrihard, A. L., Amarowicz, R., & Pegg, R. B. (2012). Phenol-based antioxidants and the in vitro methods used for their assessment. *Comprehensive Reviews in Food Science and Food Safety, 11*(2), 148–173.

Delgado-Pando, G., Cofrades, S., Ruiz-Capillas, C., Solas, M. T., & Jiménez-Colmenero, F. (2010). Healthier lipid combination oil-in-water emulsions prepared with various protein systems: an approach for development of functional meat products. *European Journal of Lipid Science and Technology, 112*, 791–801.

Di Mattia, C. D., Sacchetti, G., Mastrocola, D., & Pittia, P. (2009). Effect of phenolic antioxidants on the dispersion state and chemical stability of olive oil O/W emulsions. *Food Research International, 42*, 1163–1170.

Di Mattia, C. D., Sacchetti, G., Mastrocola, D., Sarker, D. K., & Pittia, P. (2010). Surface properties of phenolic compounds and their influence on the dispersion degree and oxidative stability of olive oil O/W emulsions. *Food Hydrocolloids, 24*(6–7), 652–658.

Ebrahimi, P., & Salmanpour, S. (2014). Topical quercetin nanoemulsions: optimization of preparation using chemometric approaches. *Pharmaceutical Chemistry Journal, 48*(6), 402–407.

Espinosa, R. R., Inchingolo, R., Alencar, S. M., Rodriguez-Estrada, M. T., & Castro, I. A. (2015). Antioxidant activity of phenolic compounds added to a functional emulsion containing omega-3 fatty acids and plant sterol esters. *Food Chemistry, 182*, 95–104.

FAO/WHO. (2010). Fats and fatty acids in human nutrition. Report of an expert consultation. *FAO Food and Nutrition Paper, 91*, 1–166.

Flaiz, L., Freire, M., Cofrades, S., Mateos, R., Weiss, J., Jiménez-Colmenero, F., et al. (2016). Comparison of simple, double and gelled double emulsions as hydroxytyrosol and n-3 fatty acid delivery systems. *Food Chemistry, 213*, 49–57.

Gomes, A., Costa, A. L. R., de Assis Perrechil, F., & da Cunha, R. L. (2016). Role of the phases composition on the incorporation of gallic acid in O/W and W/O emulsions. *Journal of Food Engineering, 168*, 205–214.

Gonçalves, V. S. S., Rodríguez-Rojo, S., De Paz, E., Mato, C., Martín, Á., & Cocero, M. J. (2015). Production of water soluble quercetin formulations by pressurized ethyl acetate-in-water emulsion technique using natural origin surfactants. *Food Hydrocolloids, 51*, 295–304.

Harika, R. K., Eilander, A., Alssema, M., Osendarp, S. J. M., & Zock, P. L. (2013). Intake of fatty acids in general populations worldwide does not meet dietary recommendations to prevent coronary heart disease: a systematic review of data from 40 countries. *Annals of Nutrition & Metabolism, 63*(3), 229–238.

Heim, K. E., Tagliaferro, A. R., & Bobilya, D. J. (2002). Flavonoid antioxidants: chemistry,

metabolism and structure-activity relationships. *The Journal of Nutritional Biochemistry, 13*(10), 572–584.
Jayasinghe, C., Gotoh, N., & Wada, S. (2013). Pro-oxidant/antioxidant behaviours of ascorbic acid, tocopherol, and plant extracts in n-3 highly unsaturated fatty acid rich oil-in-water emulsions. *Food Chemistry, 141*(3), 3077–3084.
Jiménez-Colmenero, F. (2013). Potential applications of multiple emulsions in the development of healthy and functional foods. *Food Research International, 52*(1), 64–74.
Karadag, A., Yang, X., Ozcelik, B., & Huang, Q. (2013). Optimization of preparation conditions for quercetin nanoemulsions using response surface methodology. *Journal of Agriculture and Food Chemistry, 61*(9), 2130–2139.
Kiokias, S., & Varzakas, T. (2014). Activity of flavonoids and β-carotene during the autooxidative deterioration of model food oil-in water emulsions. *Food Chemistry, 150*, 280–286.
Kiokias, S., & Varzakas, T. (2017). Innovative applications of food-related emulsions. *Critical Reviews in Food Science and Nutrition, 57*(15), 3165–3172.
Lamba, H., Sathish, K., & Sabikhi, L. (2015). Double emulsions: emerging delivery system for plant bioactives. *Food and Bioprocess Technology, 8*(4), 709–728.
Losada-Barreiro, S., Bravo-Díaz, C., & Romsted, L. S. (2015). Distributions of phenolic acid antioxidants between the interfacial and aqueous regions of corn oil emulsions: effects of pH and emulsifier concentration. *European Journal of Lipid Science and Technology, 117*(11), 1801–1813.
Losada-Barreiro, S., Sánchez-Paz, V., Bravo-Díaz, C., Paiva-Martins, F., & Romsted, L. S. (2012). Temperature and emulsifier concentration effects on gallic acid distribution in a model food emulsion. *Journal of Colloid and Interface Science, 370*(1), 73–79.
Lozano, M. V., Torrecilla, D., Torres, D., Vidal, A., Domínguez, F., & Alonso, M. J. (2008). Highly efficient system to deliver taxanes into tumor cells: docetaxel-loaded chitosan oligomer colloidal carriers. *Biomacromolecules, 9*(8), 2186–2193.
Matalanis, A., Decker, E. A., & McClements, D. J. (2012). Inhibition of lipid oxidation by encapsulation of emulsion droplets within hydrogel microspheres. *Food Chemistry, 132*(2), 766–772.
Matos, M., Gutiérrez, G., Iglesias, O., Coca, J., & Pazos, C. (2015). Enhancing encapsulation efficiency of food-grade double emulsions containing resveratrol or vitamin B12 by membrane emulsification. *Journal of Food Engineering, 166*, 212–220.
McClements, D. J. (2016). *Food emulsions : Principles, practices, and techniques/David Julian McClements* (third ed.). Boca Raton: CRC Press.
Mcclements, D. J., & Decker, E. A. (2000). Lipid oxidation in oil-in-water emulsions: impact of molecular environment on chemical reactions in heterogeneous food systems. *Journal of Food Science, 65*(8), 1270–1282.
McClements, D. J., Decker, E. A., Park, Y., & Weiss, J. (2009). Structural design principles for delivery of bioactive components in nutraceuticals and functional foods. *Critical Reviews in Food Science and Nutrition, 49*(6), 577–606.
Meddour, I., Yallese, M. A., & Aouici, H. (2015). Investigation and modeling of surface roughness of hard turned aisi 52100 steel: tool vibration consideration. In M. Haddar, M. S. Abess, J. Y. Choley, T. Boukharouba, T. Elnady, A. Kanaev, M. Ben Amar, & F. Chaari (Eds.). *Multiphysics modelling and simulation for systems design and monitoring* (pp. 425). Switzerland: Springer International Publishing.
O' Dwyer, S. P., O' Beirne, D., Ní Eidhin, D., Hennessy, A. A., & O' Kennedy, B. T. (2013). Formation, rheology and susceptibility to lipid oxidation of multiple emulsions (O/W/O) in table spreads containing omega-3 rich oils. *LWT – Food Science and Technology, 51*(2), 484–491.
O'Dwyer, S. P. O., O'Beirne, D., Ní Eidhin, D., & O'Kennedy, B. T. (2012). Effects of green tea extract and α-tocopherol on the lipid oxidation rate of omega-3 oils, incorporated into table spreads, prepared using multiple emulsion technology. *Journal of Food Science, 77*(12), N58–N65.
Orellana, S. L., Torres-Gallegos, C., Araya-Hermosilla, R., Oyarzun-Ampuero, F., & Moreno-Villoslada, I. (2015). Association efficiency of three ionic forms of oxytetracycline to cationic and anionic oil-in-water nanoemulsions analyzed by diafiltration. *Journal of Pharmaceutical Sciences, 104*(3), 1141–1152.
Poyato, C., Navarro-Blasco, I., Calvo, M. I., Cavero, R. Y., Astiasarán, I., & Ansorena, D. (2013). Oxidative stability of O/W and W/O/W emulsions: effect of lipid composition and antioxidant polarity. *Food Research International, 51*(1), 132–140.
Robert, P., García, P., Reyes, N., Chávez, J., & Santos, J. (2012). Acetylated starch and inulin as encapsulating agents of gallic acid and their release behaviour in a hydrophilic system. *Food Chemistry, 134*(1), 1–8.
Rodríguez-Carpena, J. G., Morcuende, D., & Estévez, M. (2012). Avocado, sunflower and olive oils as replacers of pork back-fat in burger patties: effect on lipid composition, oxidative stability and quality traits. *Meat Science, 90*(1), 106–115.
Romero, R., & Zuñica, L. (2005). Métodos Estadísticos en Ingeniería. 2ª edición. Ed. Univeridad Politécnica de Valencia.
Shahidi, F., & Zhong, Y. (2011). Revisiting the polar paradox theory: a critical overview. *Journal of Agriculture and Food Chemistry, 59*(8), 3499–3504.
Skurtys, O., & Aguilera, J. M. (2009). Formation of O/W macroemulsions with a circular microfluidic device using saponin and potato starch. *Food Hydrocolloids, 23*(7), 1810–1817.
Tressou, J., Moulin, P., Vergès, B., Le Guillou, C., Simon, N., & Pasteau, S. (2016). Fatty acid dietary intake in the general French population: Are the French Agency for Food, Environmental and Occupational Health & Safety (ANSES) national recommendations met? *The British Journal of Nutrition, 116*(11), 1966–1973.
UNE-EN ISO 5509:2001. Animal and vegetable fats and oils – Preparation of methyl esters of fatty acids.
Waraho, T., Cardenia, V., Decker, E. A., & McClements, D. J. (2010). Lipid oxidation in emulsified food products. *Oxidation in foods and beverages and antioxidant applications. Volume 2: Management in different industry sectors*, 306–343.
Weiss, J., & Muschiolik, G. (2007). Factors affecting the droplet size of water-in-oil-emulsions (W/O) and the oil globule size in water-in-oil-in-water emulsions (W/O/W). *Journal of Dispersion Science and Technology, 28*(5), 703–716.